

Communication: Electron impact ionization of binary $\text{H}_2\text{O}/\text{X}$ clusters in helium nanodroplets: An *ab initio* perspective

Benjamin Shepperson, Jun Liu, Andrew M. Ellis,^{a)} and Shengfu Yang^{a)}

Department of Chemistry, University of Leicester, Leicester LE1 7RH, United Kingdom

(Received 1 November 2012; accepted 19 November 2012; published online 30 November 2012)

In a recent experiment $(\text{H}_2\text{O})_n/\text{X}_m$ binary clusters (where $\text{X} = \text{Ar}, \text{N}_2, \text{CO}, \text{CO}_2$, and several other molecules) were formed in superfluid helium nanodroplets and investigated by electron impact mass spectrometry [Liu *et al.*, Phys. Chem. Chem. Phys. **13**, 13920 (2011)]. The addition of dopant X was found to affect the branching ratio between $\text{H}_3\text{O}^+(\text{H}_2\text{O})_n$ and $(\text{H}_2\text{O})_{n+2}^+$ formation. Specifically, the addition of CO increased the proportion of protonated water cluster ions, whereas dopants such as Ar, N_2 , and CO_2 , had the opposite effect. In this work *ab initio* calculations have been performed on $[\text{X}(\text{H}_2\text{O})_2]^+$ ions, where $\text{X} = \text{Ar}, \text{N}_2, \text{CO}$, and CO_2 , to try and explain this distinct behavior. CO is found to be unique in that it forms a $\text{HOCO-H}_3\text{O}^+$ unit in the most stable cationic complexes where the binding between HO and CO is stronger than that between H_3O^+ and OH . Thus, on purely energetic grounds, loss of HOCO rather than CO should be the preferred fragmentation process. No comparable chemistry occurs when $\text{X} = \text{Ar}, \text{N}_2$, or CO_2 and so the co-dopant requires less energy to depart than OH . The calculations therefore account for the experimental observations and provide evidence that HOCO formation is induced in helium droplets containing $(\text{H}_2\text{O})_n$ clusters and co-doped with CO when subject to electron impact ionization. © 2012 American Institute of Physics. [<http://dx.doi.org/10.1063/1.4769810>]

Protonated water cluster ions exhibit a rich and varied chemistry, such as proton transfer and molecular rearrangement, and various techniques, such as electron impact,¹ corona discharge,² chemical ionization,³ vacuum ultraviolet ionization,⁴ and femtosecond laser photoionization,⁵ have been applied to ionize water and form water cluster ions. It is believed that ionization first strips an electron from a single water molecule and forms a nascent water cation (H_2O^+), which dissociates rapidly through proton transfer to a neighboring water molecule. As a consequence, ionization of water results in a thermalized electron, a hydroxyl radical (OH), and a hydronium ion (H_3O^+).⁶ The latter can occur as solvated charge carriers in aqueous solutions and in protonated clusters such as $(\text{H}_2\text{O})_{20}\text{H}_3\text{O}^+$.⁷

Compared with protonated water cluster ions, unprotonated water cluster ions, $(\text{H}_2\text{O})_n^+$, have received far fewer experimental investigations. The main reason for this is that there exist large structural differences between the parent neutral clusters and their ionized counterparts, and therefore the Franck-Condon factor for adiabatic ionization is very small.^{8–10} Consequently, the ionized clusters are usually formed in highly vibrationally excited states which dissociate into $(\text{H}_2\text{O})_n\text{H}^+$ and OH ,^{8,11,12} unless the excess energy can be rapidly removed by some means.

One way to form unprotonated water cluster ions is to form cold binary clusters in a molecular beam. Shinohara *et al.* were the first to report the observation of unprotonated water cluster ions and this was achieved by applying near

threshold photoionization with an Ar resonance lamp to a supersonic expansion of H_2O and Ar.¹³ The mixed cluster ions $[(\text{H}_2\text{O})_n\text{Ar}_m]^+$ were first created, and the subsequent evaporative loss of one or more Ar atoms removed excess energy and therefore minimized OH ejection. In another set of experiments, by Dong *et al.*,¹⁴ a soft X-ray laser was used to photoionize water clusters formed using He and Ar as carrier gases. In both cases a trace of $(\text{H}_2\text{O})_2^+$ was observed but the signal was dramatically stronger when Ar was involved, presumably because Ar interacts more strongly with $(\text{H}_2\text{O})_2^+$ than He because of the higher polarizability of Ar. As a result, excess energy can be dissipated more effectively in the argon case via evaporative loss, which is compatible with the earlier findings by Shinohara.¹³

An alternative means of obtaining unprotonated water cluster ions is to ionize water clusters contained within superfluid helium nanodroplets. If electron impact is used, the initial process will almost certainly be ionization of helium, leading to He^+ , which is mobile and can ultimately transfer its charge either to the water cluster or remain on helium; helium cluster ions, He_n^+ , result in the latter case.^{15,16} If the charge is transferred to water clusters, the cold environment provided by the surrounding helium can lead to quenching of the “hot” water cluster ions so that $(\text{H}_2\text{O})_n^+$ ions can be formed and survive, which was reported first in the 1990s.^{17,18} Through similar experiments in our laboratory we have observed larger unprotonated water cluster ions with $n \leq 30$.¹⁹ More recently we formed binary clusters in helium nanodroplets by sequential addition of water and another molecular species, X (where $\text{X} = \text{O}_2, \text{N}_2, \text{Ar}, \text{CO}_2, \text{CO}, \text{NO}$, and C_6D_6).²⁰ The addition of $\text{O}_2, \text{N}_2, \text{CO}, \text{CO}_2$, and C_6D_6 to helium nanodroplets was found to increase the proportion of unprotonated water cluster

^{a)} Authors to whom correspondence should be addressed. Electronic addresses: sfyl@le.ac.uk and andrew.ellis@le.ac.uk. Telephone: +44 (0)116 252 2127. Fax: +44 (0)116 252 3789.

ions when compared with analogous experiments on pure water clusters in helium nanodroplets. On the other hand dissociative ionization, which leads to formation of $(\text{H}_2\text{O})_n\text{H}^+$ ions, was enhanced relative to the pure water case when the co-dopant was CO or NO. The decline in dissociative ionization when a co-dopant such as Ar or N_2 was added was qualitatively interpreted by an “energy in/out” mechanism.²⁰ For CO and NO co-dopants it was speculated that the increase in dissociative ionization was due to the formation of HOCO and HONO, e.g., $[(\text{H}_2\text{O})_n\text{CO}]^+ \rightarrow (\text{H}_2\text{O})_{n-1}\text{H}^+ + \text{HOCO}$. The “energy-in/out” mechanism can also be used to interpret the mass spectrum of C_{60} and water binary clusters in the recent experiments by Schöbel *et al.*,^{21,22} where the C_{60} molecules dramatically reduce the fragmentation of water clusters, leading to the dominance of unprotonated $\text{C}_{60}(\text{H}_2\text{O})_n^+$ cluster ions over protonated $\text{C}_{60}(\text{H}_2\text{O})_n\text{H}^+$ cluster ions.

In this work the results from *ab initio* calculations on $[\text{X}(\text{H}_2\text{O})_2]^+$ cluster ions are presented in order to try and understand why the branching ratio for dissociative ionization of water/X complexes can increase or decrease, depending on the identity of co-dopant X. To keep the calculations manageable and affordable, we have chosen to focus on water dimer and treat this as representative of the behavior likely for larger water clusters. For co-dopants we consider Ar, N_2 , CO, and CO_2 ; O_2 and benzene are not considered because they possess lower ionization energies than water clusters and therefore charge transfer to benzene or O_2 is expected on ionization. NO was also not included in these calculations because it possesses a lower ionization energy than water and the fragmentation of $[\text{NO}(\text{H}_2\text{O})_n]^+$ into HONO and $(\text{H}_2\text{O})_{n-1}\text{H}^+$ occurs for $n \geq 4$.²³ Our calculations focus on the binding energy of $\text{X} \cdots (\text{H}_2\text{O})_2^+$ and the influence of the co-dopant, X, on the binding energy of the $\text{HO} \cdots \text{HOH}_2^+$.

All calculations were performed at the MP2/aug-cc-pVTZ level of theory and employed GAUSSIAN 09.²⁴ Geometry optimization of the unprotonated water cluster dimer ion, $(\text{H}_2\text{O})_2^+$, was the first step and this was then used to construct the initial geometries of the various $[\text{X}(\text{H}_2\text{O})_2]^+$ ions. Previous calculations have predicted that $(\text{H}_2\text{O})_2^+$ has three possible geometries, i.e., a hydrazine-like configuration (global minimum), a gauche oriented dimer (at +0.02 eV relative to the global minimum energy) and a disproportionated ion, $\text{HO} \cdots \text{HOH}_2^+$ (+0.22 eV)^{8,25} (see Figure 1(a) for the optimized geometry of $\text{HO} \cdots \text{HOH}_2^+$). However, for reasons discussed earlier the primary ionization of water involves rapid proton transfer, leading to charge localization on an H_3O^+ moiety. As a result, the disproportionated ions are the only species that can be produced by ionization of water clusters, which has been confirmed by an Ar-tagging experiment;²⁶ hence it is unnecessary to consider other geometries of the water dimer cation in our calculation. All of the possible binding sites for X attached to $\text{HO} \cdots \text{HOH}_2^+$ were investigated. For each optimized geometry, vibrational frequency calculations were performed to confirm that a potential energy minimum is obtained. To calculate the binding energies of $\text{HO} \cdots \text{H}_3\text{O}^+$ and $(\text{H}_2\text{O})_2^+ \cdots \text{X}$, we have applied basis set superposition error (BSSE) corrections using the standard counterpoise correction procedure and the binding energy was then obtained from the formula $\Delta E_{AB} = E_{AB}$

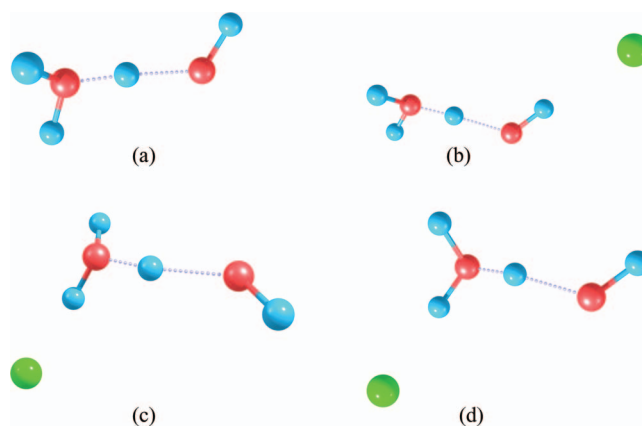


FIG. 1. Optimized geometries for (a) $\text{HO} \cdots \text{HOH}_2^+$; (b) $\text{Ar} \cdots (\text{H}_2\text{O})_2^+$; (c) *cis*- $(\text{H}_2\text{O})_2^+ \text{Ar}$; and (d) *trans*- $(\text{H}_2\text{O})_2^+ \text{Ar}$. The *trans*-geometry of $[\text{Ar}(\text{H}_2\text{O})_2]^+$, shown in (d), is the global minimum. The optimized geometries of $[\text{N}_2(\text{H}_2\text{O})_2]^+$ and $[\text{CO}_2(\text{H}_2\text{O})_2]^+$ are similar to those of $[\text{Ar}(\text{H}_2\text{O})_2]^+$, i.e., an N_2 or CO_2 molecule is attached to one of three H atoms in the dangling OH bonds.

+ BSSE - $(E_A + E_B)$,²⁷ where E_{AB} , E_A , and E_B are the total energies of molecule/cluster AB and A and B are the corresponding fragments.

For $\text{X} = \text{Ar}$, N_2 , and CO_2 , three distinct geometries were found for these binary clusters, with the co-dopant binding to one of the three free O-H bonds in each case (see Figures 1(b)–1(d) for the optimized geometries using $[\text{Ar}(\text{H}_2\text{O})_2]^+$ for illustration). The *trans* $\text{HO} \cdots \text{HOH}_2^+ \cdots \text{X}$ structure, where X is attached to the free OH bond of H_3O^+ furthest from the hydroxyl moiety, is found to be the global minimum (see Table I). The optimized global-minimum geometries of $[\text{Ar}(\text{H}_2\text{O})_2]^+$ are in good agreement with previous calculations by Gardenier *et al.*²⁶ and any slight differences are assumed to derive from the larger basis set applied in our calculations. The *cis* structure, with the X molecule attached to the dangling OH bond of H_3O^+ on the

TABLE I. The structure, total energy and binding energies of $[\text{X}(\text{H}_2\text{O})_2]^+$ ions ($\text{X} = \text{Ar}$, N_2 , CO_2 , and CO). The energies are expressed in cm^{-1} .

X	Geometries	E_{total}	$\Delta E_{\text{HO} \cdots \text{HOH}_2^+}$	$\Delta E_{(\text{H}_2\text{O})_2^+ \cdots \text{X}}$
Ar	$\text{HO} \cdots \text{HOH}_2^+ \cdots \text{Ar}$ (<i>trans</i>)	0	7811.1	1254.8
	$\text{HO} \cdots \text{HOH}_2^+ \cdots \text{Ar}$ (<i>cis</i>)	11.7	7815.7	1239.4
	$\text{Ar} \cdots \text{HO} \cdots \text{HOH}_2^+$	501.6	10103.2	790.1
N_2	$\text{HO} \cdots \text{H}_3\text{O}^+ \cdots \text{N}_2$ (<i>trans</i>)	0	7273.5	2935.4
	$\text{HO} \cdots \text{H}_3\text{O}^+ \cdots \text{N}_2$ (<i>cis</i>)	40.7	7252.3	2890.3
	$\text{N}_2 \cdots \text{HO} \cdots \text{HOH}_2^+$	872.1	11734.3	2062.9
CO_2	$\text{HO} \cdots \text{HOH}_2^+ \cdots \text{CO}_2$ (<i>trans</i>)	0	6928.5	4190.6
	$\text{HO} \cdots \text{HOH}_2^+ \cdots \text{CO}_2$ (<i>cis</i>)	25.2	6925.5	4166.4
	$\text{CO}_2 \cdots \text{HO} \cdots \text{HOH}_2^+$	1063.6	13736.4	3216.2
CO	$\text{HOCO} \cdots \text{H}_3\text{O}^+$ (<i>trans</i>)	0	7414.2	10498.1
	$\text{HOCO} \cdots \text{H}_3\text{O}^+$ (<i>cis</i>)	841.9	7848.8	9036.9
	$\text{HO} \cdots \text{HOH}_2^+ \cdots \text{CO}$ (<i>trans</i>)	6465.6	6740.7	4734.8
	$\text{HO} \cdots \text{HOH}_2^+ \cdots \text{CO}$ (<i>cis</i>)	6529.5	6706.0	4658.7
	$\text{HO} \cdots \text{HOH}_2^+ \cdots \text{OC}$ (<i>trans</i>)	8842.8	7532.3	1966.3
	$\text{HO} \cdots \text{HOH}_2^+ \cdots \text{OC}$ (<i>cis</i>)	8872.4	7515.2	1940.3
	$\text{OC} \cdots \text{HO} \cdots \text{HOH}_2^+$	7670.4	14232.8	3533.0
	$\text{CO} \cdots \text{HO} \cdots \text{HOH}_2^+$	9533.9	10881.6	1306.9

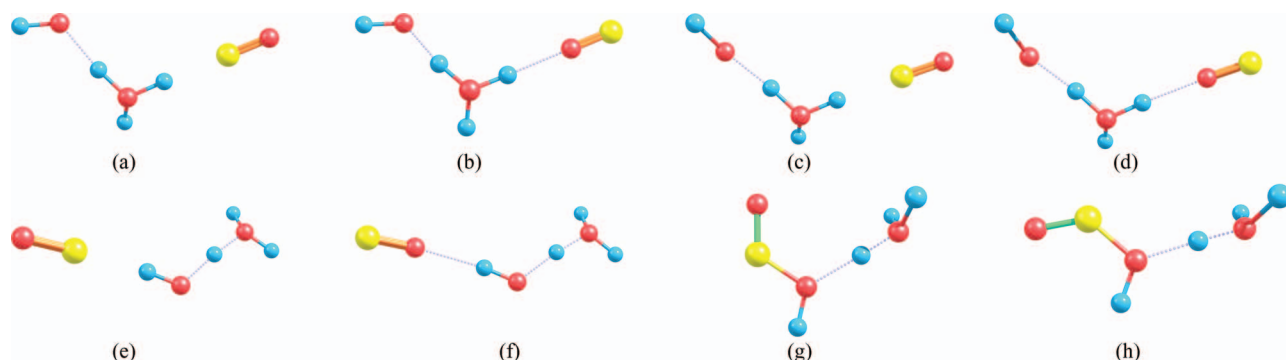


FIG. 2. Calculated structures of $[\text{CO}(\text{H}_2\text{O})_2]^+$. (a) *trans*-($\text{H}_2\text{O})_2^+ \text{CO}$; (b) *trans*-($\text{H}_2\text{O})_2^+ \text{OC}$; (c) *cis*-($\text{H}_2\text{O})_2^+ \text{CO}$; (d) *cis*-($\text{H}_2\text{O})_2^+ \text{OC}$; (e) $\text{OC} \cdots (\text{H}_2\text{O}_2)^+$; (f) $\text{CO} \cdots (\text{H}_2\text{O}_2)^+$; (g) *trans*- $\text{HOCO} \cdots \text{H}_3\text{O}^+$; (h) *cis*- $\text{HOCO} \cdots \text{H}_3\text{O}^+$.

same side as the hydroxyl moiety, is of slightly higher energy than the *trans* isomer, while the isomer with X attached to the hydroxyl moiety gives rise to the highest total energy. The difference in binding energies for the *trans* and *cis* geometries is marginal, ranging from 12 cm^{-1} to 45 cm^{-1} .

For $[\text{CO}(\text{H}_2\text{O})_2]^+$ we have found eight stable structures (see Figure 2). Both the carbon and oxygen atoms of the CO molecule can be attached to any one of the three dangling OH bonds in the $\text{HO} \cdots \text{HOH}_2^+$ ion but the lower energy structures have the carbon atom of CO attached to the oxygen atom in the hydroxyl moiety, rather than attached to hydronium ions in either the *trans* or *cis* geometry. The attaching of CO to hydroxyl produces a strong HO-CO bond, where the binding energy between CO and HO is calculated as $10\,498 \text{ cm}^{-1}$ for the *trans*-HOCO (slightly higher than the measured binding energy of neutral HOCO at 9723 cm^{-1}).²⁸ At the same time the $\text{HO} \cdots \text{HOH}_2^+$ bond strength is calculated to be 7414 cm^{-1} . The *cis*- $\text{HOCO} \cdots \text{HOH}_2^+$ ion has a slightly higher energy than the *trans* geometry, i.e., by 842 cm^{-1} , and the binding energy between CO and HO also exceeds that of the $\text{HO} \cdots \text{HOH}_2^+$ bond. The *trans* $\text{HO} \cdots \text{HOH}_2^+ \cdots \text{CO}$ ion is the third most stable structure with a much higher total energy ($+0.81 \text{ eV}$ relative to the global minimum). As seen in Table I, for $[\text{CO}(\text{H}_2\text{O})_2]^+$ at the higher energy geometries, the binding energies between CO and $(\text{H}_2\text{O})_2^+$ are always lower than that between the HO and HOH_2^+ moieties. Hence in these geometries CO will have a similar effect on $(\text{H}_2\text{O})_2^+$ as Ar, N_2 and CO_2 , i.e., biasing the branching ratio of water cluster ions toward the unprotonated ions. The increase of protonated products by the addition of CO therefore suggests an overwhelming impact of the lowest energy structures on the dissociation reactions, despite the fact that there is a large excess energy available for production of these higher energy structures following charge transfer from He^+ .

To conclude, in the most stable structures of $[\text{CO}(\text{H}_2\text{O})_2]^+$ an HOCO moiety is formed with a HO-CO binding energy exceeding that of $\text{HO} \cdots \text{HOH}_2^+$. Thus, on purely energetic grounds, any bond fission would favor cleavage of the $\text{HO} \cdots \text{HOH}_2^+$ bond rather than the loss of CO. This contrasts with water dimer cations with Ar, N_2 , or CO_2 attached, where the $\text{HO} \cdots \text{HOH}_2^+$ binding energies are always higher than the binding energy of $\text{X} \cdots (\text{H}_2\text{O})_2^+$. Thus in these cases the lowest energy dissociation process would

be loss of X, a process which would cool the remaining $(\text{H}_2\text{O})_2^+$ and thus enhance the survival probability of the unprotonated water dimer cation relative to the channel leading to $\text{H}_3\text{O}^+ + \text{OH}$. We expect that these findings will transfer to larger water clusters and they qualitatively explain the observed differences in protonated/unprotonated water cluster ion ratios seen in helium nanodroplet experiments for $\text{X}/\text{H}_2\text{O}$ co-doping.

S.Y. and A.M.E. wish to thank the UK EPSRC for a grant support on this research, and the UK National Service for Computational Chemistry Software (NSCCS) for providing the computing service.

- ¹O. Echt, D. Kreisle, M. Knapp, and E. Recknagel, *Chem. Phys. Lett.* **108**, 401 (1984).
- ²M. Okumura, L. I. Yeh, and Y. T. Lee, *J. Phys. Chem.* **94**, 3416 (1990).
- ³Z. Shi, J. V. Ford, S. Wei, and A. W. Castleman, Jr., *J. Chem. Phys.* **99**, 8009 (1993).
- ⁴L. Belau, K. R. Wilson, S. R. Leone, and M. Ahmed, *J. Phys. Chem. A* **111**, 10075 (2007).
- ⁵P. P. Radi, P. Beaud, D. Franzke, H.-M. Fray, T. Gerber, B. Mischler, and A.-P. Tzannis, *J. Chem. Phys.* **111**, 512 (1999).
- ⁶B. C. Garrett and D. A. Dixon *et al.*, *Chem. Rev.* **105**, 355 (2005).
- ⁷S. Wei, Z. Shi and A. W. J. Castleman, *J. Chem. Phys.* **94**, 3268 (1991).
- ⁸R. N. Barnett and U. Landman, *J. Phys. Chem. A* **101**, 164 (1997).
- ⁹G. S. Tshumper, M. L. Leininger, B. C. Hoffman, E. F. Valeev, H. F. Schaefer, and M. Quack, *J. Chem. Phys.* **116**, 690 (2002).
- ¹⁰S. Tomoda and K. Kimura, *Chem. Phys. Lett.* **111**, 434 (1984).
- ¹¹H. Tachikawa, *J. Phys. Chem. A* **106**, 6915 (2002).
- ¹²I. G. Gurtubay, N. D. Drummond, M. D. Towler, and R. J. Needs, *J. Chem. Phys.* **124**, 24318 (2006).
- ¹³H. Shinohara, N. Nishi, and N. Washida, *J. Chem. Phys.* **84**, 5561 (1986).
- ¹⁴F. Dong, S. Heinbush, J. J. Rocca, and E. R. Bernstein, *J. Chem. Phys.* **124**, 224319 (2006).
- ¹⁵W. K. Lewis, M. Lindsay, R. J. Bemish, and R. E. Miller, *J. Am. Chem. Soc.* **127**, 7235 (2005).
- ¹⁶A. M. Ellis and S. Yang, *Phys. Rev. A* **76**, 032714 (2007).
- ¹⁷M. Lewerenz, B. Schilling, and J. P. Toennies, *J. Chem. Phys.* **102**, 8191 (1995).
- ¹⁸R. Fröchtenicht, M. Kaloudis, M. Koch, and F. Huisken, *J. Chem. Phys.* **105**, 6128 (1996).
- ¹⁹S. Yang, S. M. Brereton, S. Nandhra, A. M. Ellis, B. Shang, L. Yuan, and J. Yang, *J. Chem. Phys.* **127**, 134303 (2007).
- ²⁰J. Liu, B. Shepperson, A. M. Ellis, and S. Yang, *Phys. Chem. Chem. Phys.* **13**, 13920 (2011).
- ²¹S. Denifl, F. Zappa, I. Mähr, F. Ferreira da Silva, A. Aleem, A. Mauracher, M. Probst, J. Urban, P. Mach, A. Bacher, O. Echt, T. D. Märk, and P. Scheier, *Angew. Chem., Int. Ed.* **48**, 8940 (2009).

- ²²S. Denifl, F. Zappa, I. Mähr, A. Mauracher, M. Probst, J. Urban, P. Mach, A. Bacher, D. K. Bohme, O. Echt, T. D. Märk, and P. Scheier, *J. Chem. Phys.* **132**, 234307 (2010).
- ²³A. J. Stace, J. F. Winkel, R. B. Lopez Martens, and J. E. Upham, *J. Phys. Chem.* **98**, 2012 (1994).
- ²⁴M. J. Frisch, G. W. Trucks, H. B. Schlegel *et al.*, GAUSSIAN 03, Revision C.02, Gaussian, Inc., Wallingford, CT, 2004.
- ²⁵S. P. de Visser, L. J. de Koning, and N. M. M. Nibbering, *J. Phys. Chem.* **99**, 15444 (1995).
- ²⁶G. H. Gardenier, M. A. Johnson, and A. B. McCoy, *J. Phys. Chem. A* **113**, 4772 (2009).
- ²⁷C. J. Cramer, *Essentials of Computational Chemistry: Theories and Models*, 2nd ed. (Wiley, 2004).
- ²⁸B. Ruscic and M. Litorja, *Chem. Phys. Lett.* **316**, 45 (2000).